



# Analyzing two-dimensional tunable photonic crystal waveguides for communication band optical filter applications

Durga Rama Pavan Vadapalli<sup>1</sup> · Sourabh Roy<sup>1</sup>

Received: 19 February 2020 / Accepted: 7 June 2021 / Published online: 23 June 2021  
© The Optical Society of India 2021

**Abstract** A two-dimensional photonic crystal waveguide with thermally tunable photonic bandgap is proposed. The tunability of the photonic bandgap is achieved by the temperature dependence of the refractive index of the slab. A hexagonal lattice with a lattice shift is used as a two-dimensional photonic crystal waveguide. The shift of the innermost rows just adjacent to the waveguide resulted with a larger bandgap. To study the temperature dependence of PBG, the refractive index variations are considered over the temperature range of 100–400 K. The bandgap is controlled by the temperature of the slab, and the photonic bandgap values ranging from 24 to 58 nm are achieved. The work is extended in the communication bands including O-band, E-band, S-band, C-band and L-band. The simulations are performed in MIT Photonic Bands software. Thermally tunable optical filters, wavelength routers, optical interconnectors and temperature sensors can be realized from these results.

**Keywords** Photonic crystal waveguides · Tunable photonic bandgap · Optical filters · MPB method

## Introduction

The growth in computational power demands compact and on-chip optical interconnectors, optical filters, switches and optical routers. Due to the properties like maximum confinement of light, compact size and working frequency,

photonic crystal waveguides (PCW) are becoming a better choice for various light controlling applications [1].

PCWs are the periodic structures that possess photonic bandgap (PBG) and behave as an insulator in the forbidden frequency bands [2, 3]. PBG of a PCW originates from destructive interference of multiple reflections of light, and this is due to its geometry and refractive index (RI) of the material from which it is fabricated [2]. They have received enormous interest from the scientific community due to their light controlling abilities in second harmonic generation, third harmonic generation, routing of electromagnetic radiation, slowdown of light, optical interconnectors, optical switches and wavelength filters [4–10]. Compact size and fabrication methods from the existing technologies made them popular in light controlling applications [11–13]. In recent studies, it is found that the tuning of PBG can enhance these light controlling applications [14–17]. These studies resulted in tunable PBG for different applications like optical interconnectors, terahertz filters, optical shutters, reflectors, wavelength-tunable lasers and sensors [14, 18–23]. Yet, till the recent past, PBG remains unaltered.

The tuning of the PBG can be done either passively or actively. If the desired PBG is achieved via altering the geometry, RI of the material and profile of the RI, then it is called passive tuning. In this method, once the structure is fabricated, the PBG is fixed. These methods limit the devices as static devices. On the other side, using methods like external electric field, magnetic field, incorporating liquid crystals (LC) and changing waveguide's temperature can cause slight changes in the RI of the material and shifts the PBG up to desired range. This is active tuning of the PBG and has potential applications in the real-time light controlling devices.

✉ Sourabh Roy  
sroy@nitw.ac.in

<sup>1</sup> Department of Physics, National Institute of Technology, Warangal 506004, India

In the recent past, tunability of the PBG was achieved by the arrangement of layers of one-dimensional PC in different types of quasi-periodic sequences which resulted with tunable PBG in the terahertz region for various applications [23]. In these structures, grading RI profile and temperature effects were adopted to achieve tunability. This is also achieved in one-dimensional photonic crystals (PC) using linear graded-index materials [24]. Here, maximum contrast in the RI results in higher bandwidths. Recently, the geometry of the PC structure is altered by lithographic techniques to achieve tunability of PBG [25]. In this method, a laser wavelength was tuned from 1500 to 1625 nm using a monolithic semiconductor wafer as the active medium. Geometrical width of the PCW is altered to achieve the tuning of the waveguide modes [26].

Even though the above methods are tuning the PBG, they provide limited applications due to passive tuning. PCs made of ferroelectric, ferromagnetic and ferrimagnetic materials offer considerable active tuning of PBG in the moderate external electric or magnetic field [27]. Tunable PBG was achieved by inserting LCs and single-crystal  $\text{KTaO}_3$  in the PC matrix and upon applying heat or external electric field [14, 15, 18, 22]. Tuning was attained in omnidirectional terahertz range PCs by external temperature effect [19]. The tunability was realized from the temperature dependence of the constituent semiconductor and dielectric elements. With the effect of temperature on free carrier charge density and by the density of dopants, tunability of PBG was reported [28]. By the external control of temperature, even the PBG can be closed in this method. However, among all the methods, thermal tuning of the PCW provides relatively larger tunability in the PBG and efficiency in tuning. Even though these methods propose tunability of PBG structures, yet this remains a less explored area.

In the present work, we report the thermal tuning of the PBG in a two-dimensional lattice-shifted hexagonal-based PCW. The shift in PCW is generally used to establish the dispersion engineering. Here, this method was used to enhance the PBG for wavelength filtering application. The tunability was achieved by thermal tuning of the RI of Gallium Arsenide (GaAs). Temperatures ranging from 100 to 400 K were considered for this purpose. In most of the recent results one-dimensional PC and PCW were tuned using thermal methods to achieve the tunable PBG. In two-dimensional PC and PCW, using LC resulted in the tuning. In the present work, thermal tuning was directly implemented in two-dimensional PCW for tunable PBG. Relatively larger temperature ranges were used than the existing results. Simulations are performed in MIT Photonic Bands (MPB) software (open source) on Ubuntu platform. This work attained the PBG ranging from 24 to 58 nm with a tuning range of 20–34 nm in the communication bands.

These studies can lead to the development of thermally active wavelength filter using PCW.

### Theory and methods

#### (i) Tuning of RI

As per thermo-optic effect, the RI of a material alters as a function of temperature. McCaulley et al. [29] discussed the temperature dependence of the RI of GaAs in the near-infrared region, which is given by

$$n(T) = n(T_{\text{ref}}) \cdot \exp[(T - T_{\text{ref}})\beta] \tag{1}$$

where  $n(T)$  represents the RI of GaAs at temperature  $T$ ,  $n(T_{\text{ref}})$  is the RI of GaAs at a reference temperature  $T_{\text{ref}}$  and  $\beta$  is the thermo-optic coefficient of GaAs. Here, for all the wavelengths,  $T_{\text{ref}}$  is chosen as 300 K and  $\beta$  is taken as  $2.25 \times 10^{-4} \text{ K}^{-1}$ . Using Eq. (1), the RI of GaAs is calculated in the range of 100–400 K temperatures in the near-infrared regions including O-band, E-band, S-band, C-band and L-band with central wavelengths 1.31, 1.41, 1.50, 1.55 and 1.59  $\mu\text{m}$ , respectively. The plot in Fig. 1 shows the variation of RI against the chosen temperature range at different communication bands.

These calculated RI values are used during the simulations in MPB. The simulations are performed to calculate the band positions and the PBG of the lattice-shifted PCW.

#### (ii) Modes in PCW

Although PC and PCW structures are mixed dielectric media, propagation of light in them obeys the well-known macroscopic Maxwell's equations. Different regions of a PCW with homogeneous dielectric material can be mapped with a position vector  $\vec{r}$ . To solve such equations for PCW

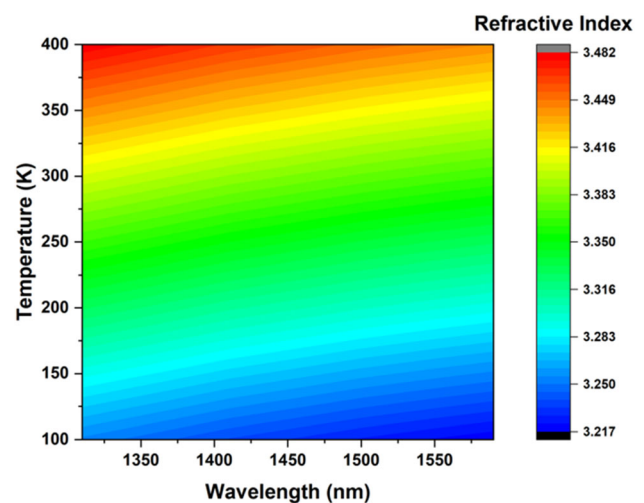


Fig. 1 Variation of RI of GaAs with the temperature at different communication bands

structures, one can consider the following assumptions including no free charge carriers or currents are present inside the structure, it doesn't vary with time, the field strengths are small and the medium is lossless. By these assumptions, one can modify the Maxwell's equations and find the electric and magnetic fields associated with the structure.

In general, these fields depend on both space and time. However as the Maxwell's equations are linear, the time dependence can be separated from the spatial dependence. It results the equations for light propagation in PCW structures and those are known as harmonic modes or states of the system. For obtaining the fields with spatial dependence only, one can write the harmonic modes as complex-valued fields and then pick-up only the real part. By writing the harmonic mode as a product of spatial pattern and a complex exponential, it is given by [30]

$$\vec{H}(\vec{r}, t) = \vec{H}(\vec{r})e^{-i\omega t} \text{ and } \vec{E}(\vec{r}, t) = \vec{E}(\vec{r})e^{-i\omega t}. \quad (2)$$

Substituting the above equations in Maxwell's equations and solving them result with fields in spatial domain, given by [30]

$$\nabla \times \vec{E}(\vec{r}) - i\omega\mu_0\vec{H}(\vec{r}) = 0 \text{ and } \nabla \times \vec{H}(\vec{r}) + i\omega\epsilon_0\epsilon(\vec{r})\vec{E}(\vec{r}) = 0. \quad (3)$$

By coupling the above two equations and eliminating  $\vec{E}$ , one can get an equation containing only  $\vec{H}$  which is given by

$$\nabla \times \left( \frac{1}{\epsilon(\vec{r})} \nabla \times \vec{H}(\vec{r}) \right) = \left( \frac{\omega}{c} \right)^2 \vec{H}(\vec{r}). \quad (4)$$

Due to the symmetry in PCWs, the electromagnetic modes can be written as Bloch states. To adopt the Bloch's theorem, a periodic function  $\vec{u}(\vec{r})$  must be defined and it is considered here as  $\vec{u}(\vec{r}) = \vec{u}(\vec{r} + \vec{R})$  for all lattice vectors  $\vec{R}$ . And then the existing Bloch state in the structure can be written as  $\vec{H}(\vec{r}) = \exp[i\vec{k} \cdot \vec{r}] \vec{u}(\vec{r})$ . By substituting this expression in Eq. (4) and solving, one can calculate the eigenstates existing in the PCW. In the present case, MPB is used on the Ubuntu platform for performing the simulations. Similarly, one can eliminate  $\vec{H}$  from Eq. (3) and obtain an equation consisting only  $\vec{E}$ .

(iii) Geometrical parameters of the structure

The proposed structure is designed aiming tunable PBG with controlled dispersion. The propagation of waves in a medium depends on the dispersion. The dispersion in waveguides can be controlled by tailoring its geometry [31]. With this idea, the geometrical parameters are chosen to control the dispersion that exists in PCW. The existing

literature suggests that the radius of air cylinders ( $r$ ) in the range of  $0.22a$ – $0.28a$  with slab thickness ( $h$ ) of  $0.4a$ – $0.5a$  provides control over dispersion [32, 33] where 'a' is the lattice constant of the structure. Though varying the air cylinder radius results in the modification of the dispersion curve, controlling the radius of air cylinders and producing systematic variations are difficult. Displacement in the row of air cylinders also provides dispersion control and can be useful in developing slow light PCW [32, 33]. Also, the displacement of air cylinders is preferable over the variation of their radius. This lattice-shift factor ( $s$ ) can be in the range of  $0.12a$ – $0.18a$  [32, 33].

As the displacement of the row of air cylinders is also affecting the PBG, to select the suitable displacement factor, simulations were performed at  $1310 \mu\text{m}$  wavelength and considering the PCW at 300 K temperature. Figure 2 shows the variations in the PBG of the proposed structure with a lattice shift. This study suggests that the increase in lattice shift offers larger PBG. Hence, the lattice-shift factor ( $s$ ) is chosen as  $0.18a$ .

(iv) Studying the tunability of PBG

To study the temperature effect on the PBG, the PBG of the proposed structure is calculated at temperatures ranging from 100 to 400 K in the communication bands. For doing this, using Eq. (1) the RI values and the dielectric constants of GaAs are calculated at the chosen temperature range. These values are used in the simulations performed in MPB. From the obtained results, the band diagram of the structure is plotted. With these data, the PBG of the PCW is calculated at every temperature step. The shift in bands due to temperature is plotted at different communication bands. To realize the structure at different communication bands, the lattice constant values are calculated and the corresponding eigenwavelengths are determined. The effect of

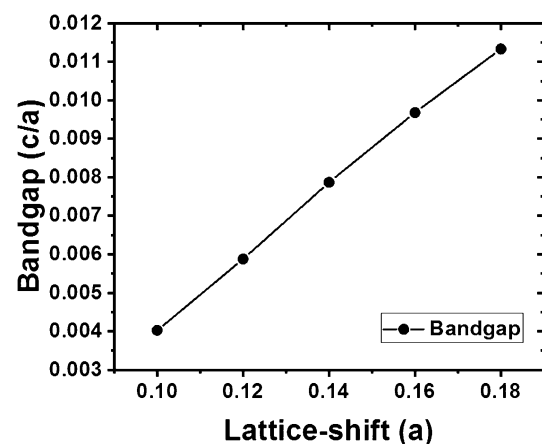


Fig. 2 Variation of PBG with lattice shift. This is performed at  $1310 \mu\text{m}$  wavelength and 300 K temperature

temperature on PBG is plotted at these calculated lattice constants.

### Schematic of the waveguide

For achieving the tunability of the PBG in the PCW, a symmetrical PCW with hexagonal lattice is considered. Seven rows of air cylinders are considered on both sides of the line-defect. This defect structure can confine the light that propagates through it, whose frequency is within the range of the PBG. The geometrical parameters of the slab including thickness ( $h$ ), radius of air cylinders ( $r$ ) and width of the line-defect ( $w$ ) are chosen as  $0.383a$ ,  $0.25a$  and  $0.86a$ , respectively. The innermost row of the air cylinders, just adjacent to the line-defect are moved away by  $0.18a$  for achieving larger PBG. The schematic of the proposed structure is shown in Fig. 3.

The micro-heater plates can be connected to an electronic driving circuit to keep the slab at a particular temperature. This induces the change in RI of the slab via thermo-optic effect, and the tuning of the PBG can be observed.

### Results and discussion

#### (i) Bandgap of the structure

The simulations performed in MPB resulted with eigenfrequencies and band positions of the structure. Using these data, the band diagram is obtained for the proposed structure. Initially, the studies are performed at the temperature of 300 K. The band diagram of the proposed structure is obtained at wavelengths 1.31, 1.41, 1.50, 1.55 and 1.59  $\mu\text{m}$  corresponding to O-band, E-band, S-band, C-band and L-band, respectively. Figure 4 shows the band diagram of the proposed lattice-shifted PCW structure at 1.55  $\mu\text{m}$  wavelength and 300 K temperature.

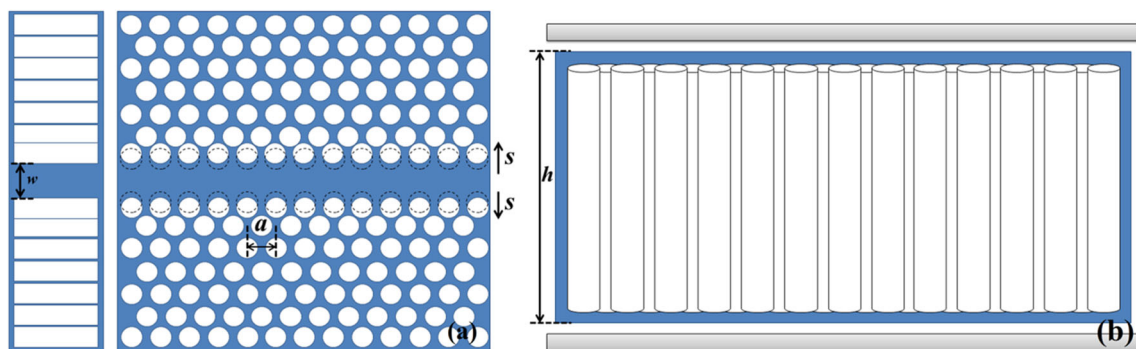


**Fig. 3** The proposed lattice-shifted waveguide with hexagonal lattice. **a** Top and side view of the structure. **b** The proposed structure with micro-heater plates for temperature control

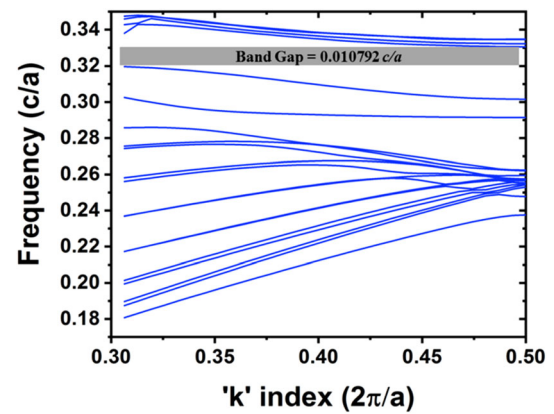


**Fig. 4** Band diagram of the PCW at 1.55  $\mu\text{m}$  wavelength and 300 K temperature

The obtained results show that the bandgap for this structure exists between band 16 and 17. Similarly, the simulations are performed at other chosen wavelengths to obtain the band structure.

Table 1 shows the bandgap of the structure at 300 K across various communication bands.

By calculating the lattice constant of the structure, one can get the absolute value of the PBG. Obtained eigenfrequencies, eigenwavelengths and bandgap conforms the presence of PBG in the near-infrared region. For the above structure, the lattice constant varies in the range of 440–520 nm to observe bandgap in the near-infrared region. Existing technology supports the fabrication of PCW with these geometrical parameters [33].

#### (ii) Tuning the PBG

Simulations are performed to study the effect of temperature on PBG and tunable photonic structures. For this, the temperature range is chosen as 100–400 K. Using Eq. (1), the RI of the GaAs slab is calculated at wavelengths 1.31, 1.41, 1.50, 1.55 and 1.59  $\mu\text{m}$ . And these calculated RI values are used during the simulation. The positions of band 16 and band 17 are noted at every



**Table 1** PBG of the structure at 300 K temperature

Communication band	Position of band 16 (units of $c/a$ )	Position of band 17 (units of $c/a$ )	Bandgap (units of $c/a$ )
O-band (1.31 $\mu\text{m}$ )	0.316727	0.32806	0.011333
E-band (1.41 $\mu\text{m}$ )	0.31817	0.329353	0.011183
S-band (1.50 $\mu\text{m}$ )	0.319227	0.33007	0.010843
C-band (1.55 $\mu\text{m}$ )	0.319714	0.330506	0.010792
L-band (1.59 $\mu\text{m}$ )	0.320078	0.330831	0.010753

temperature interval and at selected wavelengths. As expected, the bands are shifting with temperature. Using these data, the bandgap is calculated and confirmed the shift in PBG with temperature. As we are interested in the positions of band 16 and band 17, only these two bands are plotted against the  $k$ -index of the structure at different temperatures. For instance, Fig. 5 shows the variations of band 16 and band 17 at 1.55  $\mu\text{m}$  wavelength with temperature.

From these data, the bandgap of the structure is calculated at every temperature interval and at selected wavelengths. The change in bandgap is observed with temperature and Fig. 6 shows these variations.

The PBG arises from the geometry of the PCW. To study the effect of the thermal expansion on the PBG, the structure is simulated without and with considering thermal expansion of the material. It is found that thermal expansion of GaAs doesn't affect the PBG as it is negligible in the magnitude. Yet, for other materials, thermal expansion may also affect the PBG with temperature. Therefore, shift in the bandgap in the present case is due to the changes in the RI, which is emerging from the thermo-optic effect. Hence, a plot is drawn to integrate the changes in the bandgap with the RI variations and it is shown in Fig. 7.

(iii) Calculating the lattice constants

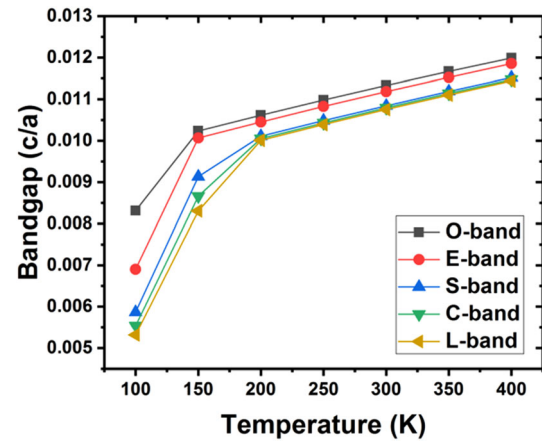


**Fig. 6** Shift in bandgap with change in temperature

As the obtained results are having the units in terms of 'c' and 'a,' for realizing the structures, lattice constant values are calculated. Table 2 shows the PBG of the structures at different temperatures with calculated lattice constants.

Figure 8 shows the variations in the PBG with the change in temperature for the above calculated lattice constant values. At the lower temperatures, these bandgap

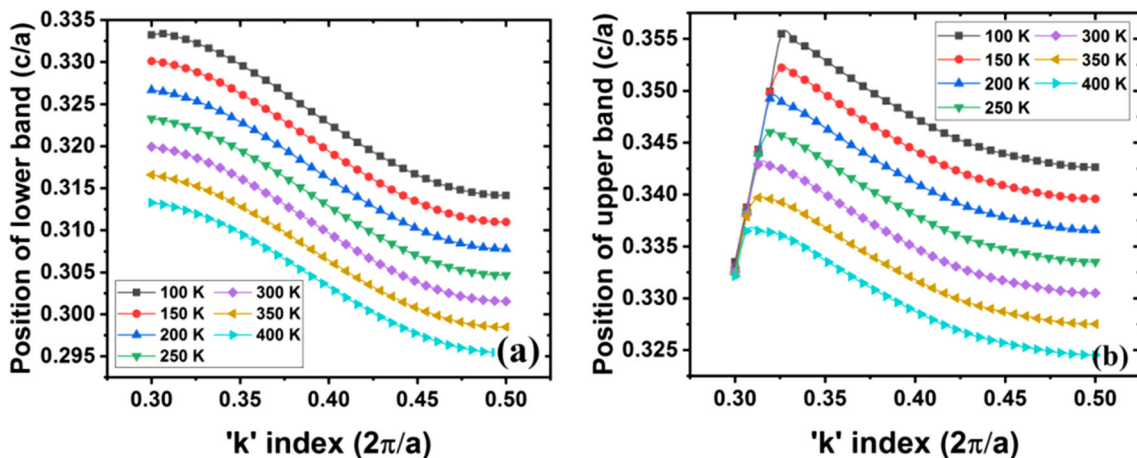


**Fig. 5** Shift in the position of bands with temperature at 1.55  $\mu\text{m}$  wavelength: **a** Band 16 and **b** Band 17

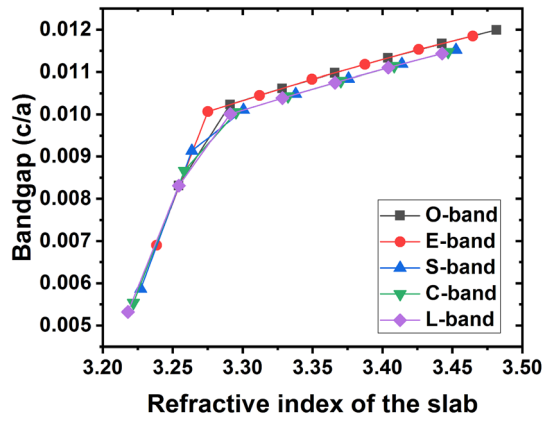


Fig. 7 Variation of bandgap with RI of the slab

variations are very sharp and at the higher temperatures, the change is relatively small.

It is clear that the bandgap is increasing with the rise in temperature. Here, the lattice constant values are carefully selected so that the desired bands fall in the communication bands and confine the desired wavelengths. However, it is essential to investigate different methods for quick heating and cooling of the structure to use it in the applications like filtering and routing of the wavelengths. This PCW can also be used as a temperature sensor with a relatively larger response time, which may limit its applications in real-time temperature monitoring.

(iv) Dispersion analysis

The inverse of the first-order dispersion is referred as group velocity. And the group index is a measure of group velocity of light in the waveguide. Figure 9 shows the variation of group index with wavelength, calculated at the band 16 of the waveguide at different temperatures. Second-order dispersion ( $\beta_2$ ) was calculated using the group index and is plotted in Fig. 10. The nonlinear behavior and

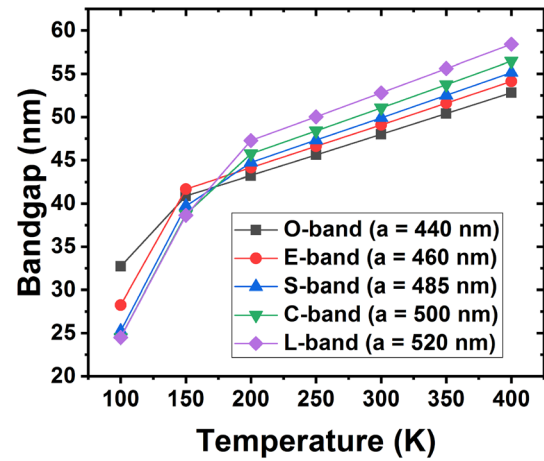


Fig. 8 Variation of bandgap with change in temperature at different wavelengths and lattice constants

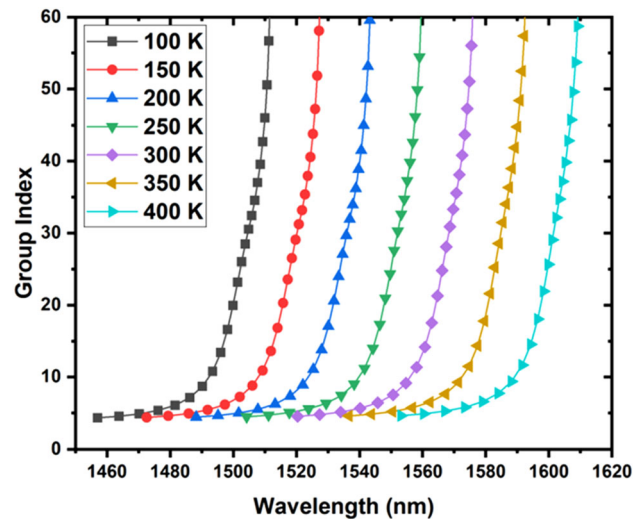
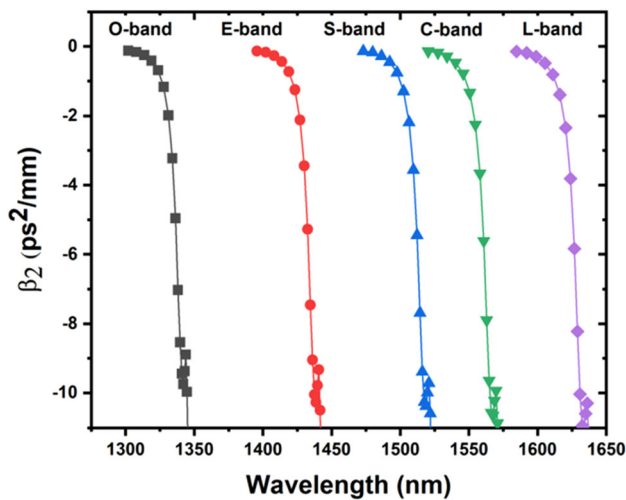


Fig. 9 Variation of group index with wavelength at different temperatures

Table 2 PBG of the structure at different communication bands and at different temperatures

Temperature (K)	Calculated PBG (nm)				
	$a = 440$ nm and in O-band	$a = 460$ nm and in E-band	$a = 485$ nm and in S-band	$a = 500$ nm and in C-band	$a = 520$ nm and in L-band
100	32.71	28.26	25.24	24.52	24.49
150	40.88	41.68	39.71	38.76	38.63
200	43.23	44.13	44.74	45.74	47.28
250	45.60	46.60	47.31	48.39	50.03
300	47.99	49.09	49.91	51.07	52.80
350	50.40	51.60	52.52	53.75	55.60
400	52.82	54.13	55.15	56.47	58.42



**Fig. 10** Second-order dispersion ( $\beta_2$ ) calculated at 300 K temperature

the dispersion characteristics of the waveguide can be estimated from these graphs.

From Fig. 10, it can be observed that the magnitude of  $\beta_2$  is of the order of  $10^{-22}$  s<sup>2</sup>/m or of the order of ps<sup>2</sup>/mm, which is an acceptable range for the applications based on PC and PCW. In all the communication bands and at all the temperatures, the  $\beta_2$  is in the permissible range. This confirms the possible application of the wavelength filtering with low dispersion at the selected communication band.

## Conclusions

In conclusion, we have shown that the PBG of a two-dimensional PCW can be tunable using thermo-optic effect. This is resulted with tunable PBG ranging from 24 to 58 nm with a shift of about 34 nm. Tunability is achieved by introducing temperature dependence of RI of GaAs in the range of 100–400 K. The tunable structures are developed for all communication bands. To realize the effect of temperature, the PBG is plotted against the temperature of the PCW. For realizing the structure, the lattice constants are calculated for all communication bands. The dispersion analysis confirms the lower dispersion at the selected wavelengths. These tunable PBG structures can be used in optical filters, wavelength routers, optical shutters, dynamic detectors and interconnectors. This may also help in the development of on-chip integrated circuits due to their small size and material compatibility.

**Acknowledgements** The authors sincerely thank Department of Science and Technology, Government of India for funding this work through the INSPIRE fellowship (IF160435).

## References

1. C.M. Soukoulis, *Photonic Crystals and Light Localization in the 21st Century* (Kluwer Academic, London, 2012)
2. J.D. Joannopoulos, P.R. Villeneuve, S. Fan, Photonic crystals: putting a new twist on light. *Nature* **386**, 143–149 (1997)
3. M. Notomi, Theory of light propagation in strongly modulated photonic crystals: Refractionlike behavior in the vicinity of the photonic band gap. *Phys. Rev. B* **62**, 10696–10705 (2000)
4. R.G. Zaporozhchenko, Second harmonic generation in photonic-crystal one-dimensional media. *Quantum Electron.* **32**, 49–53 (2002)
5. B. Corcoran, C. Monat, C. Grillet, D.J. Moss, B.J. Eggleton, T.P. White, L. O’Faolain, T.F. Krauss, Green light emission in silicon through slow-light enhanced third-harmonic generation in photonic-crystal waveguides. *Nat. Photon.* **3**, 206–210 (2009)
6. A.M. Apetrei, J.M. Moison, J.A. Levenson, M. Foroni, F. Poli, A. Cucinotta, S. Selleri, M. Legre, M. Wegmüller, N. Gisin, K.V. Dukelskii, A.V. Khokhlov, V.S. Shevandin, Y.N. KondratEv, C. Sibilia, E.E. Serebryannikov, A.M. Zheltikov, Electromagnetic field confined and tailored with a few air holes in a photonic-crystal fiber. *Appl. Phys. B* **81**, 409–414 (2005)
7. T. Baba, Slow light in photonic crystals. *Nat. Photon.* **2**, 465–473 (2008)
8. Y. Zhang, B. Li, Photonic crystal-based bending waveguides for optical interconnections. *Opt. Express* **14**, 5723–5732 (2006)
9. T. Tanabe, M. Notomi, S. Mitsugi, A. Shinya, E. Kuramochi, All-optical switches on a silicon chip realized using photonic crystal nanocavities. *Appl. Phys. Lett.* **87**, 151112 (2005)
10. N. Mattiucci, G. D’Aguanno, M. Scalora, M.J. Bloemer, Cross-phase modulation in one-dimensional photonic crystals: applications to all-optical devices. *Appl. Phys. B* **81**, 389–391 (2005)
11. G. Recio-Sanchez, Z. Dang, V. Torres-Costa, M.B.H. Breese, R.J. Martin-Palma, Highly flexible method for the fabrication of photonic crystal slabs based on the selective formation of porous silicon. *Nanoscale Res. Lett.* **7**, 449 (2012)
12. H.C. Guo, D. Nau, A. Radke, X.P. Zhang, J. Stodolka, X.L. Yang, S.G. Tikhodeev, N.A. Gippius, H. Giessen, Large-area metallic photonic crystal fabrication with interference lithography and dry etching. *Appl. Phys. B* **81**, 271–275 (2005)
13. M. Campbell, D.N. Sharp, M.T. Harrison, R.G. Denning, A.J. Turberfield, Fabrication of photonic crystals for the visible spectrum by holographic lithography. *Nature* **404**, 53–56 (2000)
14. S.M. Weiss, M. Haurylau, P.M. Fauchet, Tunable photonic bandgap structures for optical interconnects. *Opt. Mater.* **27**, 740–744 (2005)
15. D.M. Pustai, A. Sharkawy, S. Shi, D.W. Prather, Tunable photonic crystal microcavities. *Appl. Opt.* **41**, 5574–5579 (2007)
16. J. Cos, J. Ferre-Borrull, J. Pallares, L.F. Marsal, Analysis of tunable bandgaps in liquid crystal-infiltrated 2D silicon photonic crystals. *Appl. Phys. B* **100**, 833–839 (2010)
17. J. Hwang, M.H. Song, B. Park, S. Nishimura, T. Toyooka, J.W. Wu, Y. Takahashi, K. Ishikawa, H. Takezoe, Electro-tunable optical diode based on photonic bandgap liquid-crystal heterojunctions. *Nat. Mater.* **4**, 383–387 (2005)
18. H. Nemeč, L. Duvillaret, F. Garet, P. Kuzel, P. Xavier, J. Richard, D. Raully, Thermally tunable filter for terahertz range based on a one-dimensional photonic crystal with a defect. *J. Appl. Phys.* **96**, 4072–4075 (2004)
19. X. Dai, Y. Xiang, S. Wen, H. He, Thermally tunable and omnidirectional terahertz photonic bandgap in the one-dimensional photonic crystals containing semiconductor InSb. *J. Appl. Phys.* **109**, 053104 (2011)

20. Y. Chen, C. Zhang, Y. Zhu, S. Zhu, N. Ming, Tunable photonic crystals with superconductor constituents. *Mater. Lett.* **55**, 12–16 (2002)
21. S.K. Srivastava, M. Upadhyay, S.K. Awasthi, S.P. Ojha, Tunable reflection bands and defect modes in one-dimensional tilted photonic crystal structure. *Opt. Photonics J.* **02**, 230–236 (2012)
22. R. Ozaki, T. Matsui, M. Ozaki, K. Yoshino, Electrically color-tunable defect mode lasing in one-dimensional photonic-band-gap system containing liquid crystal. *Appl. Phys. Lett.* **82**, 3593–3595 (2003)
23. B.K. Singh, P.C. Pandey, Tunable temperature-dependent THz photonic bandgaps and localization mode engineering in 1D periodic and quasi-periodic structures with graded-index materials and InSb. *Appl. Opt.* **57**, 8171–8181 (2018)
24. B.K. Singh, P. Kumar, P.C. Pandey, Tunable photonic band-gaps in one-dimensional photonic crystals containing linear graded index material. *Appl. Phys. B* **117**, 947–956 (2014)
25. O. Painter, A. Husain, A. Scherer, P.T. Lee, I. Kim, J.D. O'Brien, P.D. Dapkus, Lithographic tuning of a two-dimensional photonic crystal laser array. *IEEE Photon. Technol. Lett.* **12**, 1126–1128 (2000)
26. M. Notomi, A. Shinya, K. Yamada, J.I. Takahashi, C. Takahashi, I. Yokohama, Structural tuning of guiding modes of line-defect waveguides of silicon-on-insulator photonic crystal slabs. *IEEE J. Quantum Electron.* **38**, 736–742 (2002)
27. A. Figotin, Y.A. Godin, I. Vitebsky, Two-dimensional tunable photonic crystals. *Phys. Rev. B* **57**, 2841–2848 (1998)
28. P. Halevi, F. Ramos-Mendieta, Tunable photonic crystals with semiconducting constituents. *Phys. Rev. Lett.* **85**, 1875–1878 (2000)
29. J.A. Mccaulley, V.M. Donnelly, M. Vernon, I. Taha, Temperature dependence of the near-infrared refractive index of silicon, gallium arsenide, and indium phosphide. *Phys. Rev. B* **49**, 7408–7417 (1994)
30. J.D. Joannopoulos, S.G. Johnson, J.N. Winn, R.D. Meade, *Photonic Crystals: Molding the Flow of Light* (Princeton University Press, Princeton, 2008)
31. L. Yin, Q. Lin, G.P. Agrawal, Dispersion tailoring and soliton propagation in silicon waveguides. *Opt. Lett.* **31**, 1295–1297 (2006)
32. P. Colman, S. Combrie, G. Lehoucq, A.D. Rossi, Control of dispersion in photonic crystal waveguides using group symmetry theory. *Opt. Express* **20**, 13108–13114 (2012)
33. J. Li, T.P. White, L. O'Faolain, A. Gomez-Iglesias, T.F. Krauss, Systematic design of flat band slow light in photonic crystal waveguides. *Opt Express* **16**, 6227–6232 (2008)

**Publisher's Note** Springer Nature remains neutral with regard to jurisdictional claims in published maps and institutional affiliations.